ACS APPLIED MATERIALS & INTERFACES

Research Article

www.acsami.org

Effects of Zero-Length and Non-Zero-Length Cross-Linking Reagents on the Optical Spectral Properties and Structures of Collagen Hydrogels

Yu-Jer Hwang, Joseph Granelli, and Julia Lyubovitsky*

University of Califorina at Riverside, Riverside, California

Supporting Information

ABSTRACT: We compared the effects of zero-length cross-linkers 1-ethyl-3 (3dimethylaminopropyl) carbodiimide (EDC) and non-zero-length cross-linkers glycolaldehyde and glyceraldehyde on the optical and structural properties of three-dimensional (3D) collagen hydrogels. We evaluated these effects by multiphoton microscopy (MPM) that combined two-photon fluorescence (TPF) and second harmonic generation (SHG) contrasts and transmission electron microscopy (TEM). The collagen hydrogels were incubated separately with the above-mentioned reagents present at the concentration of 0.1 M. The incubation with glycolaldehyde and glyceraldehyde induced strong autofluorescence within the gels. We followed the formation of fluorescence with TPF signals *in situ* and in real time as well as characterized the micro- and nanostructures within cross-linked hydrogels by examining SHG and TEM images respectively. As detected in the SHG images, glycolaldehyde- and glyceraldehyde-modified 5−10 μm "fiberlike" collagen structures to longer, 20 μm and more, aggregated strands while EDC had minimal effect on the microstructure. TEM revealed that glycolaldehyde and glyceraldehyde either completely eliminated collagen's characteristic native fibrillar striations or generated uncharacteristic fibrils with extensions. EDC preserved the native striation patterns, decreased the fibril diameters and effectively homogenized the fibrils within hydrogels assembled at 1.8−4.68 g/L collagen concentrations and 37 °C. Our findings provide a clear understanding on how different cross-linking reagents have very different effects on the collagen hydrogels. This understanding is critical for advancing tissue engineering and wound healing applications.

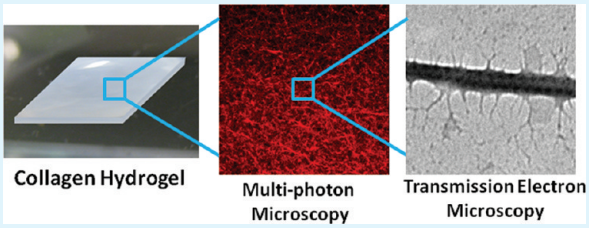

KEYWORDS: *collagen, hydrogel, cross-linking, glycation, carbodiimide, glyceraldehyde, glycoaldehyde, multiphoton, microscopy*

INTRODUCTION

Collagen hydrogels are natural biomaterials known for their biocompatibility and low cytotoxicity. However, for tissue engineering applications, collagen hydrogels need to be more mechanically stable and durable, which led to the use of various cross-linking reagents (CLR) to strengthen them. In spite of many CLRs routinely employed to stabilize collagen-based scaffolds, their effect on the optical spectral properties and hierarchical structure of collagen within scaffolds has not been systematically investigated. To understand the effects of CLRs on the optical properties and structures within the collagen-based hydrogels, it is necessary to investigate the correlation between different reagents and collagen hierarchical structure.

In this study, we compared the effects of zero-length cross-linker 1-ethyl-3 (3-dimethylaminopropyl) carbodiimide (EDC) and the non-zero-length cross-linkers glyceraldehyde and glycolaldehyde on the optical and structural properties of three-dimensional (3D) collagen hydrogels. The study was set to investigate how these two different types of cross-linking reagents influence collagen hierarchical organization ranging from the micro- to nanoscale. This goal was accomplished by employing multiphoton microscopy (MPM) to examine the production of two-photon fluorescence (TPF) within collagen microstructure, excitation wavelength dependence of TPF as well as the microstructure itself via second harmonic generation (SHG) contrast; transmission electron microscopy (TEM) was used to evaluate changes in the collagen nanostructure.

Water-soluble carbodiimide EDC is a common zero-length cross-linker, which has been utilized to modify collagen,[1−17] gelatin,[18−21] fibrinogen,[22] and chitosan.[23,24] Cross-linking of proteins with EDC results in the formation of the amide bonds and because carbodiimide does not become a part of the final protein conjugate, this cross-linking reagent was defined as zero-length. Glyceraldehyde and glycolaldehyde are the glycation reagents and produce non-zero-length cross-linking.[25−30] The glycation begins with a Maillard reaction during which an amino group of the protein reacts with a carbonyl group of sugar. Upon several subsequent reactions and rearrangements, the sugars become incorporated into the protein conjugate to form adducts collectively known as advanced glycated end-products (AGEs). AGEs from various

Received: September 26, 2011
Accepted: December 1, 2011
Published: December 1, 2011

tissues had been long thought to absorb in the near-UV (320−370 nm) and fluoresce in the 380−460 nm range.[31]

EXPERIMENTAL SECTION

Collagen Materials Formation and Cross-Linking. Soluble rat-tail type I collagen, 8.58 mg/mL (BD Biosciences) was dissolved in 0.02 N acetic acid. The purity of this stock solution was verified with 4%-20% Tris-HCl gels (Bio-Rad) following a standard protocol. The stock solution was diluted with 0.02 N acetic acid to obtain the 2× collagen aliquots. 2× initiation buffers were prepared from NaCl and phosphate buffer. The concentration of mono and dibasic phosphate in the buffer at pH 7.4 were calculated with Henderson−Hasselbalch equation. The pH was adjusted dropwise with 1N NaOH or HCl. Ionic strength was adjusted with NaCl. The initiation buffer had the following components: 6.40 g/L K_2HPO_4; 3.16 g/L KH_2PO_4; 38.55 g/L NaCl (ionic strength = 0.6 M). After the pH was adjusted to a desired value, the initiation buffer was filtered with 0.22 μm, 25 mm syringe filter (Fisher) and stored at 4 °C. Prior to the beginning of material formation, both 2X collagen stock and initiation buffer were deairated by placing in a 1.5 L desiccator (Fisher) and applying house vacuum for 2 h. Material formation was initiated by mixing 2× collagen aliquot with 2× initiation buffer on ice at 1:1 ratio, verifying the pH to be 7.4 ± 0.1, and then incubated at 37 °C. The final collagen concentration of the materials is 2 mg/mL unless noted. For multiphoton microscopy and confocal microscopy measurements collagen materials were prepared in 8-well chambered coverglass (MP Biomedicals). For one-photon experiments, collagen materials were prepared in 96-well plates (BD Falcon). In both cases, after 24 h incubation at 37 °C, the materials were incubated in 0.1 M glyceraldehyde, 0.1 M glycolaldehyde, 0.1 M EDC, and 0.1 M EDC/.025 M NHS solutions (Sigma) at the same temperature for the specified times.

Multiphoton Microscopy (MPM) and Spectroscopy. The inverted multiphoton laser scanning microscope used in this work was the Zeiss LSM 510 NLO Meta microscopy system. It is based on an Axiovert 200 M inverted microscope equipped with standard illumination systems for transmitted light and epi-fluorescence detection. It was also equipped with an NLO interface for a femtosecond titanium: sapphire laser excitation source (Chameleon-Ultra, Coherent, Incorporated, Santa Clara, CA) for multiphoton excitation. The Chameleon laser provided femtosecond pulses at a repetition rate of about 80 MHz, with the center frequency tunable from 690 to 1040 nm. A long working distance objective (Zeiss, 40× water, N.A. 0.8) was used to acquire images shown in this work. The two-photon signals from the samples were epi-collected and discriminated by the short pass 650 nm dichroic beamsplitter. The SHG and TPF images were collected using the META detection module with the signals sampled in a 375−415 nm and 470−500 nm detection range respectively (λ_{ex} = 800 nm). Each image presented in this work is 12 bit, 512 × 512 pixels representing 225 μm × 225 μm field of view. All the experiments were repeated on separate days, using up to 8 independent samples on each day (about 5 fields of view per sample). The upright multiphoton laser-scanning microscope used to acquire spectra was the modified Zeiss Axioexaminer.Z1. It was equipped with a femtosecond titanium:sapphire laser excitation source (Mai-Tai HP, Spectra Physics, Santa Clara, CA) that provided femtosecond pulses at a repetition rate of about 80 MHz, with the center frequency tunable from 690 to 1040 nm. A long working distance objective (Zeiss, 10× water, N.A. 0.3) was used to acquire spectra. The two-photon signals generated by the samples were epi-collected, discriminated by a long pass 665 nm single-edge dichroic beamsplitter and filtered through a 720 nm short pass filter. Spectra were obtained with a Acton SP2300 spectrograph equipped with a 68 mm × 68 mm 300 grooves/mm ruled grating blazed at 500 nm and a Pixis1024B CCD camera (Princeton Instruments, Trenton, New Jersey). The spectrograph and camera settings were PC-controlled through WinSpec/32 v.2.5K software. The CCD temperature was maintained at −75 °C for all the experiments to ensure low dark noise. The entrance slit of the spectrograph was set to a width of 0.5 mm. The typical spectral acquisition time was 4 s. The multiphoton spectra were corrected for the nonlinearity of the laser excitation power, quantum efficiency of the CCD camera, and dark noise background.

Transmission Electron Microscopy (TEM) Imaging. After 24 h of incubation, an entire portion of an incubated sample was retrieved. A drop of sample containing cross-linked material was added on a Formvar film coated with a layer of carbon supported on a 300-mesh copper grid (Carbon type A, Ted Pella, Inc.). Excess liquid was drained with filter paper after 10 min. A drop of double deionized water was then added to the sample on the grid for 1 s to remove the excess NaCl, and was drained slowly with filter paper. A drop of same-day-prepared 10 g/L sodium phosphotungstate (Sigma), pH 7.4 was added to the sample on the grid. After 5 min of staining, the grid was drained slowly with filter paper. A drop of double deionized water was then added to the sample on the grid for 1 s to remove the excess stain and then air-dried for about 15 min. The grids were examined immediately in a Tecnail 12 electron microscope operated at 120 kV.

RESULTS AND DISCUSSION

The reaction between carbodiimide and proteins follows the mechanism expressed in Figure 1A. The carboxyl groups of

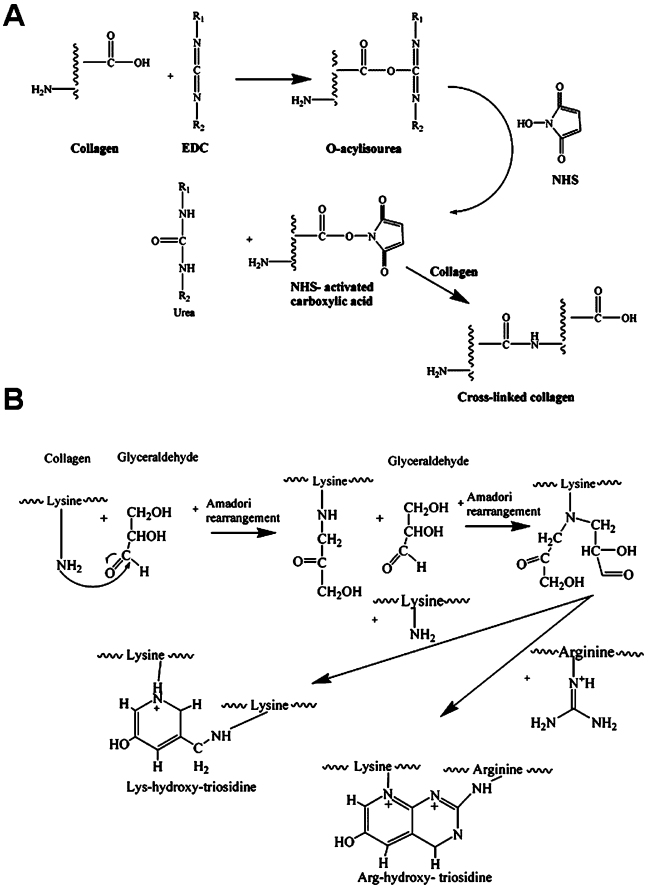

Figure 1. Schematics for the cross-linking reaction of collagen with (A) 1-ethyl-3 (3-dimethylaminopropyl) carbodiimide (EDC) and (B) glyceraldehyde.

aspartic or glutamic acid side chains in collagen react with this compound to form an activated O-acylurea. This intermediate can then react with a neighboring amino group of lysine side chain of collagen to form an amide bond while releasing urea derivative of the reagent.[32] However, because O-acylurea is susceptible to hydrolysis in the aqueous physiological solutions, the insufficient stability of this intermediate decreases the overall efficiency of the cross-linking reaction. The addition of

N-hydroxysuccinimide (NHS), which reacts through O-acylurea to form a more hydrolysis resistant compared to O-acylurea amine-reactive ester, increases the yield of carbodiimide cross-linking.[33]

On the other hand, the highly reactive sugars glyceraldehyde and glycoaldehyde cross-link proteins through a Millard reaction. Figure 1B shows a possible collagen cross-linking mechanism with the glyceraldehyde that involves two glyceraldehyde molecules as proposed in ref 34. In that work, the major fluorescent products detected from the incubation of glyceraldehyde with N^{α}acetyl-L-lysine and N^{α}-acetyl-L-arginine were lys-hydroxytriosidine (LHT), which is the lysine−lysine cross-link and arg-hydroxy-triosidine (AHT), which is the arginine-lysine cross-link. LHT and AHT structures shown in Figure 1B were also detected in human and porcine corneas treated with glyceraldehyde. Figure S1 in the Supporting Information expresses the possible mechanism for collagen cross-linking by glycoaldehyde. Similar to modification with the glyceraldehyde, it involves a Schiff base adduct. The subsequent Amadori rearrangement generates a new aldehyde function in a form of an aldoamine leading to pirazine formation and covalent cross-linking of collagen.[35,36] The fluorescent structures, however, have not been unequivocally identified.

In situ Microscopic Characterization of Cross-Linked Collagen Hydrogels: Two-Photon Fluorescence (TPF) and Second Harmonic Generation (SHG). To examine the effect of cross-linking on microstructure of collagen hydrogels, we employed multiphoton microscopy. TPF signals are utilized to monitor the extent of cross-linking and SHG signals are used to identify the microstructure of collagen fibers.

Generally, we find that it is useful to initially obtain TPF spectra of our modified hydrogels prior to visualizing fluorescent structures with the multiphoton microscope. This approach aids in setting the appropriate filters to collect the TPF signals that can be used to generate TPF images at a specific excitation wavelength. The TPF spectra acquired on the glycated samples (Figure 2) illustrated that 800 nm excitation wavelength generated glycation induced TPF centered at approximately 485 nm and that the 470−500 nm range of emission wavelengths set for the detection of TPF signals would be suitable. As seen in Figure 2, the TPF spectrum undergoes a bathochromic (red) shift when the excitation wavelength is changed from 720 to 800 nm, whereas no appreciable fluorescence can be excited with 900 nm light. This wavelength dependent shift of the multiphoton fluorescence spectra agrees with a trend previously reported by our group[37] for the one-photon fluorescence spectra of the fluorophores generated upon glycating collagen hydrogels.

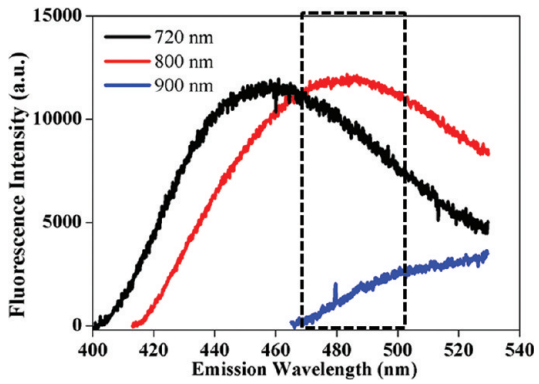

Figure 2. Two-photon fluorescence (TPF) spectrum of glyceraldehyde treated collagen hydrogels excited with different wavelengths. The rectangle indicates the range of emission wavelength that was set for the detection of TPF signals in this study.

To follow the extent of cross-linking with glycation reagents, we monitored the fluorescence intensity throughout the course of glycation via the excitation with 800 nm light. The evolution of two-photon fluorescence was detected in X-Y plain through a 470—500 nm filter as shown in Figure 2. No fluorescence was detected before the addition of sugars (Figure 3A). When the incubation reached 48 h, elongated and very strongly fluorescing structures were present (Figure 3B). The long fluorescent structures would get even longer after 1 month of incubation (Figure 3C). It is notable that TPF of the glyceraldehyde-induced cross-links has soft appearance without clear edges and extends into the background. The spectrally and structurally similar development of fluorescence was observed when the samples were treated with glycolaldehyde instead of glyceraldehydes. As judged from the kinetic profiles obtained by detecting one-photon fluorescence intensity, the reaction between the glycolaldehyde and collagen was approximately two times faster compared to the one between glyceraldehyde and collagen.

To identify if the original fiber structure within collagen hydrogels was modified due to glycation, we acquired the second harmonic generation (SHG) images at the same time as TPF images using the same 800 nm excitation wavelengths. As seen in SHG images, glycation reagents clearly modified the original microstructure of fibers in collagen hydrogels. The short fibers with length approximately 5−10 μm were observed within hydrogels prior to glycation (Figure 3D). After 48 h of glycation, few short fibers were modified to become longer fibers with length approximately 20 μm (Figure 3E). The formation of these longer fibers was even more evident when the hydrogels were allowed to react with glycation reagents for 1 month (Figure 3F). Interestingly, the SHG generated by collagen fibers did not simply colocalize with the induced TPF signals. In the TPF images, there were some fluorescent structures, which did not have the corresponding structure in the SHG image. These newly formed fluorescent structures are possibly the linkages between adjacent fibrils, which do not contribute to the SHG generating features.

Upon detecting with multiphoton microscopy the significant changes to the microstructure within collagen hydrogels induced by glycation reagents, we proceeded to examine the effects of EDC and EDC/NHS on the microstructure of collagen hydrogels as well.

Because EDC or EDC/NHS does not generate any fluorescence when they react with collagen, only the SHG signal was detected. The SHG images clearly showed that a modification of collagen hydrogels with EDC did not cause a significant alteration to the microstructure (Figure 4B). The microstructure of the EDC-modified samples appeared similar to the controls consisting of samples without the addition of any EDC (Figure 4A). Upon addition of NHS, the microstructure of fibers remained very similar to those cross-linked with EDC only (Figure 4C).

The application of SHG and TPF signals can be successfully utilized to characterize the glycation effect. These two signals show that sugars significantly modify both: the spectral optical properties and the microscopic architecture within collagen hydrogels. On the other hand, EDC has no effect on the

dx.doi.org/10.1021/am2013147 | ACS Appl. Mater. Interfaces 2012, 4, 261−267

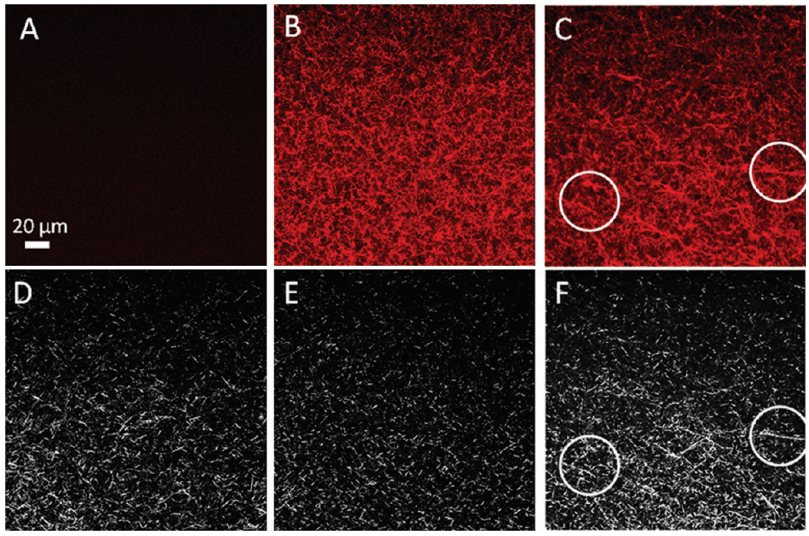

Figure 3. Typical two-photon fluorescence (TPF) and second harmonic generation (SHG) images of a sample incubated with 100 mM glyceraldehyde for a different amount of time. The images are taken in XY plane. TPF, (A) 0 h, (B) 48 h, and (C) 4 weeks; SHG, (D) 0 h, (E) 48 h, and (F) 4 weeks. Formation of the long, aggregated strands with length longer than 20 μm can be seen in the TPF and SHG images within the areas circled with the white outline. The collagen concentration of the sample is 2.0 mg/mL and the incubation temperature is 37 °C. The scale bar is 20 μm. The filters for SHG and TPF are 375−415 nm and 470−500 nm, respectively. The excitation wavelength is 800 nm.

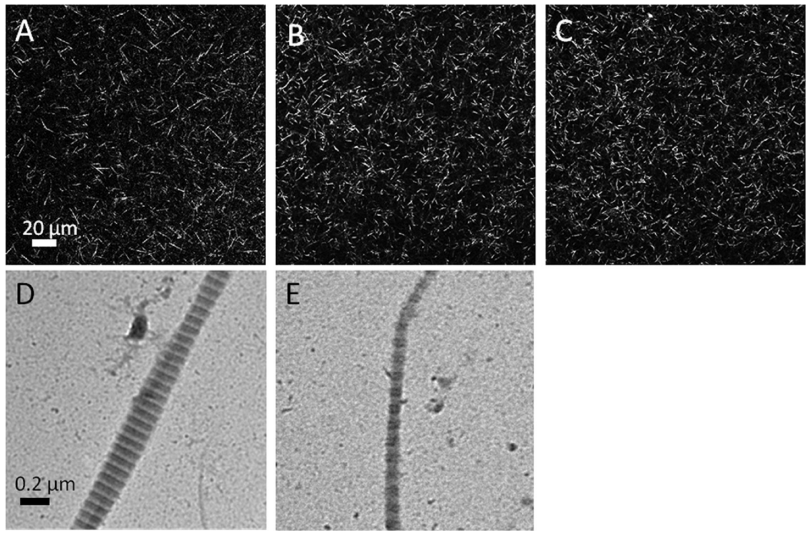

Figure 4. Typical second harmonic generation (SHG) and transmission electron microscopy (TEM) images of a sample incubated with 100 mM EDC or 100 mM EDC/25 mM NHS. The images are taken in XY plane. SHG, (A) collagen hydrogels only, (B) collagen hydrogels treated with EDC and (C) collagen hydrogels treated with EDC/NHS; TEM, (D) collagen hydrogels only, (E) collagen hydrogels treated with EDC. The collagen concentration of the sample is 2.0 mg/mL and the incubation temperature is 37 °C. The scale bar is 20 μm for SHG and 0.2 μm for TEM.

collagen structures at the microscopic level of organization and does not alter the spectral optical properties of collagen hydrogels.

We believe that the significant differences in which sugars and EDC affect the microstructure within collagen hydrogels can be attributed to the differences in their cross-linking mechanisms. The glycation occurs both intra- and intermolecularly, resulting in sugars becoming integral parts of the cross-linked structures collectively known as advanced glycation endproducts (AGEs). The newly created AGE bridges perhaps then exert certain forces that aggregate the nearby fibrils into a longer "fiberlike" feature. It is interesting that although the fiber grows in length, the diameter of the fiber remains roughly the same. Our observation would imply that the previously detected with medium angle X-rays[38] highly directional lateral expansion of the collagen unit cell at the molecular level remarkably extends to the microscopic structures within our hydrogels as well. In this earlier X-ray work, specific glycation-induced cross-links were thought to be primarily responsible for the expansion of the unit cell because they push the collagen molecules apart and away from the cross-link sites, allowing water to enter the structure in response.

On the other hand, EDC induces only the formation of amide bonds within and between collagen molecules without introducing any additional chemical moieties. Even if these newly established amide bonds could cause expansion of the collagen unit cell at the molecular level, it does not appear to extend to the microscopic scale to a visually detectable degree. As a result, the microstructure within EDC cross-linked

hydrogels as determined from visualizing SHG signals is maintained.

The near-infrared wavelength of light utilized in our two-photon fluorescence (TPF) and second harmonic generation (SHG) imaging is nondestructive to collagen 3D hydrogels. A combination of TPF and SHG imaging can provide high-contrast, three-dimensional microstructural details regarding the effects of cross-linking within these soft biomaterials. At this time, there are not many studies in the literature that had relied on the optical properties of the collagen hydrogels to obtain microstructural details. Our nondestructive observations on the effect of glycating collagen within hydrogels clearly show the significant changes to the microstructure introduced by the glycation.[37] The other optical studies are, however, less clear concerning the effects of modifying the structures within collagen-based scaffolds with the glycation reagents. For example, the 40% decrease in the SHG signal when the human tendon was glycated[39] was previously observed and could be interpreted as some change of structure. A reflectance confocal microscopy study showed the microstructure remaining unchanged in the collagen gels glycated with glucose-6-phosphate.[26] EDC not having any effect on the microstructure within collagen hydrogels is well-shown in our SHG images presented in this work, whereas no relevant previous optical imaging characterization was located.

Characterization of Cross-Linked Collagen Hydrogels with Transmission Electron Microscopy. We used transmission electron microscopy to determine if in addition to their effect on the microstructure, the cross-linking reagents affect the nanostructure of collagen fibrils within hydrogels as well. The TEM images show that EDC did not alter much of the nanostructure of collagen fibrils. The collagen fibrils treated with EDC (Figure 4E) maintained the nativelike striation with D periods ranged from 62 to 67 nm (Figure 4D). However, on the basis of the histograms constructed from TEM image measurements, we detected a decrease in the fibril diameters (Figure 5A) and a decrease in the fibril diameter distribution

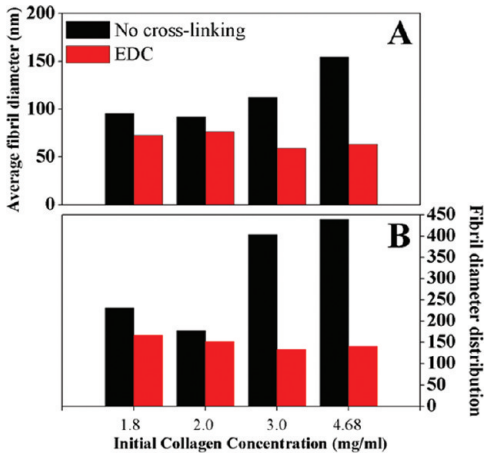

Figure 5. Effect of 100 mM EDC on the average collagen fibril diameters and fibril diameter distribution. (A) Average fibril diameter. (B) Fibril diameter distributions.

(Figure 5B) within EDC-treated collagen hydrogels. The apparent homogenization in the fibrillar diameters upon EDC-treating hydrogels assembled from different initial collagen concentrations was observed. The previous investigations are less clear concerning the effects of modifying the structures within protein-based scaffolds with EDC. For example, when electrospun fibrinogen scaffolds were treated with EDC, scanning electron microscopy studies showed no change in morphology and pore size compared to untreated controls.[22] Another study that used transmission electron microscopy[10] showed that EDC treatment of amniotic membranes causes aggregation of collagen fibers at certain EDC concentrations while leaving the rest of the structure unchanged.

As opposed to the modification done by EDC, the TEM images show that the glycation reagents significantly altered the nanostructures of collagen fibrils. When collagen hydrogels were treated with either glyceraldehyde or glycolaldehyde, collagen fibrils with native striation patterns (Figure 6A) could no longer be observed. Instead, the only nanostructures we were able to detect in the glycated samples were the nonstriated filaments (Figure 6B) and uncharacteristic fibrils with thin fibrous extensions emanating from them (Figure 6C).

Our previous work demonstrated that the nonstriated filaments can occur within 3D collagen hydrogels assembled at the initial collagen concentrations and incubation temperatures used in this work.[40] In filaments, collagen molecules are not assembled in staggered alignment and the distance between them might be too close for the phosphotungstate stain to enter; hence, filaments do not exhibit banding patterns. We believe that the disruption of the banding patterns is exuberated by glycation. We could not locate any prior TEM record of uncharacteristic fibrils with fibrous extensions emanating from them that we observed in our glycated hydrogels. We speculate that the thin fibrous extensions are the bridging cross-links that held together larger fibrillar structures disrupted by smearing the samples on the grids for the TEM visualization. These findings are in good agreement with most studies that recognized the ultrastructural changes within various glycated collagen-based tissues and materials. Scanning force microscopy work revealed structural alterations in the radii and cleft depth of tendons incubated with 0.5 M glucose for 2 weeks and detected connections between the fibrils.[41] The medium-angle X-ray diffraction studies[38] detected changes in collagen molecular packing within tendons exposed to reducing sugars, when rat tail tendons were incubated in 0.2 M ribose. The electron micrographs of tendons' cross sections showed an increased fibril packing density, fusion of fibrils and irregular fibril diameters.[23] Scanning electron microscopy study showed an apparent increase in the number of large pores (diameters >12.5 nm) in the bovine kidney tubular basement membrane treated with glucose.[38]

In short, our TEM images indicate that two sugars (glyceraldehyde and glycolaldehyde) acted on collagen hydrogels to either completely remove the striation patterns within fibrils or to transform the remaining fibrils to develop uncharacteristic extension. On the other hand, treatment with EDC reduced the fibril diameters, but maintained the native fibrillar striation patterns. On the basis of the cross-linking mechanism of sugars in which the sugar molecules incorporate into the final protein-conjugated product, this intra- and intermolecular incorporation likely to disrupt the native staggered alignment of collagen molecules within collagen fibrils thus altering the striation patterns. On the other hand, because EDC does not become part of the final cross-linking products, the striation pattern is preserved.

dx.doi.org/10.1021/am2013147 | ACS Appl. Mater. Interfaces 2012, 4, 261–267

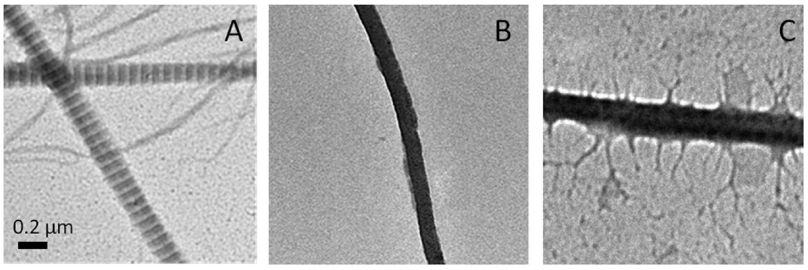

Figure 6. Transmission electron micrographs of negatively stained collagen fibrils cross-linked with 100 mM glyceraldehyde. (A) Typical collagen fibril with native banding observed in nontreated control samples. (B) Typical nonstriated filaments observed in the glyceraldehyde treated samples and (C) Collagen uncharacteristic fibrils observed in the glyceraldehyde treated samples. The scale bar is 0.2 μm.

CONCLUSION

This study investigated the effects of zero-length cross-linker EDC and non-zero-length cross-linker glycolaldehyde and glyceraldehyde on the optical and structural properties of 3D collagen hydrogels. As was seen in our studies, these two different groups of cross-linking reagents imposed very different effects on the collagen hydrogels. As detected in the SHG images, EDC did not alter the short fiber microstructure, whereas both sugars modified the short collagen fibers to longer once. The TEM images illustrated that EDC reduced the fibrillar diameter although it preserved the fibrillar striation patterns, whereas both sugars either completely eliminate the striation patterns within collagen fibrils or caused formation of very uncharacteristic fibrils with hanging fibrous nanostructures. Overall, this study is a comprehensive understanding of the effects of different kinds of cross-linking reagents. The results will potentially benefit tissue engineering, wound healing, and food research. Moreover, because the physical interaction between cells and extracellular matrix are known to affect the cell fate, our finding provide a way to easily modify the structure of the matrix either in nano- or microscale to benefit of design of the proper environment for target cells.

ASSOCIATED CONTENT

Supporting Information

Supplementary Figure S1 expresses the possible mechanism for collagen cross-linking by glycoaldehyde. This material is available free of charge via Internet at http://pubs.acs.org/

AUTHOR INFORMATION

Corresponding Author

*E-mail: julial@ucr.edu.

ACKNOWLEDGMENTS

The work was supported by the UC Riverside startup research funds (J.G.L.), the NSF CAREER Award CBET-0847070 (J.G.L), and NSF BRIGE Award EEC-0927297 (J.G.L.). We also thank Prof. Bruce J. Tromberg for access to a Zeiss LSM 510 NLO Meta microscopy system at UC Irvine supported under the Laser Microbeam and Medical Program (LAMMP), a NIH Biomedical Technology Resource, Grant P41-RR01192, at the University of California, Irvine.

REFERENCES

(1) Cao, H.; Xu, S. *J. Mater. Sci.: Mater. Med.* **2008**, *19*, 567−575.
(2) Davidenko, N.; Campbell, J. J.; Thian, E. S.; Watson, C. J. *Acta Biomater.* **2010**, *6*, 3857−3968.
(3) Duan, X.; Sheardonw, H. *J. Biomed. Mater. Res. Part A* **2005**, *75A*, 510−518.
(4) Duan, X.; Sheardonw, H. *Biomaterials* **2006**, *27*, 4608−4617.
(5) Gong, Z.; Xiong, H.; Long, X.; Wei, L.; Li, J.; Wu, Y.; Lin, Z. *Biomed. Mater.* **2010**, *5*.
(6) Jorege-Herrero, E.; Fonseca, C.; Barge, A. P.; Turnay, J.; Olmo, N.; Fernandez, P.; Lizarbe, M. A.; Paez, J. M. G. *Artif. Organs* **2010**, *34*, 168−176.
(7) Keogh, M. B.; O'Brien, F. J.; Daly, J. S. *Acta Biomater.* **2010**, *6*, 4305−4313.
(8) Lai, E. S.; Anderson, C. M.; Fuller, G. G. *Acta Biomater.* **2011**, *7*, 2448−2456.
(9) Liu, Y.; Gan, L.; Carlsson, D. J.; Fagerbolm, P.; Lagali, N.; Watsky, M. A.; Munger, R.; Hodge, W. G.; Priest, D.; Griffith, M. *Invest. Ophthalmol. Visual Sci.* **2006**, *47*, 1869−1875.
(10) Ma, D.; Lai, J.; Cheng, H.; Tsai, C.; Yeh, L. *Biomaterials* **2010**, *31*, 6647−6658.
(11) Madhavan, K.; Belchenko, D.; Motta, A.; Tan, W. *Acta Biomater.* **2010**, *6*, 1413−1422.
(12) McLaughlin, C. R.; Acosta, M. C.; Luna, C.; Liu, W.; Belmonte, C.; MGriffith, M.; Gallar, J. *Biomaterials* **2010**, *31*, 2770−2778.
(13) Nagai, N.; Mori, K.; Munekata, M. *J. Biomater. Appl.* **2008**, *23*, 275−287.
(14) Tan, G.; Dinnes, D. L. M.; Cooper-White, J. J. *Acta Biomater.* **2011**, *7*, 2804−2816.
(15) Yahyouche, A.; Zhidao, X.; Czernuszka, J. T.; Clover, A. J. P. *Acta Biomater.* **2011**, *7*, 278−286.
(16) Yao, L.; Biliar, K. L.; Winderbank, A. J.; Pandit, A. *Tissue Eng. PT. C-Meth.* **2010**, *16*, 1585−1596.
(17) Yunoki, S.; Mori, K.; Suzuki, T.; Nagai, N.; Munekata, M. *J. Mater. Sci.: Mater. Med.* **2007**, *18*, 1369−1375.
(18) Kuijpers, A. J.; Engers, G. H. M.; Feijen, J.; De Smedt, S. C.; Meyvis, T. K. L.; Demeester, J.; Krijgsveld, J.; Zaat, S. A. J.; Dankert, J. *Macromolecules* **1999**, *32*, 3325−3333.
(19) Lai, J.; Li, Y. *Mater. Sci. Eng.* **2010**, *30*, 677−685.
(20) Lai, J.; Li, Y. *J. Biomater. Sci.* **2011**, *22*, 277−295.
(21) Ratanavaraporn, J.; Rangkupan, R.; Jeeratawatchai, H.; Kanokpanaont, S.; Damrongsakkul, S. *Int. J. Biol. Macromol.* **2010**, *47*, 431−438.
(22) Sell, S. A.; Francis, M. P.; Garg, K.; McClure, M. J.; Simpson, D. G.; Bowlin, G. L. *Biomed. Mater.* **2008**, *3*.
(23) Custodio, C. A.; Alves, C. M.; R.L., R.; Mano, J. F. *J. Tissue Eng. Regener. Med.* **2010**, *4*, 316−323.
(24) Xu, H.; Yan, Y.; Li, S. *Biomaterials* **2011**, *32*, 4506−4516.
(25) Danilov, N. A.; Ignatieva, N. Y.; Iomdina, E. N.; Semenova, S. A.; Rudenskaya, G. N.; Grokhovskaya, T. E.; Lunin, V. V. *Biochim. Biophys. Acta* **2008**, *1780*, 764−772.
(26) Francis-Sedlak, M. E.; Uriel, S.; Larson, J. C.; PGreisler, H. P.; Venerus, D. C.; Brey, E. M. *Biomaterials* **2009**, *30*, 1851−1856.
(27) Girton, T. S.; Oegema, T. R.; Grassl, E. D.; Isenberg, B. C.; Tranquillo, R. T. *ASME* **2000**, *122*, 216−223.
(28) Girton, T. S.; Oegema, T. R.; Tranquillo, R. T. *J. Biomed. Mater. Res.* **1998**, *46*, 87−92.
(29) Reddy, G. K. *Exp. Diabetes Res.* **2004**, *5*, 143−153.
(30) Wollensak, G.; Iomdina, E. *Acta Ophthalmol.* **2008**, *86*, 887−893.

(31) Fujimori, E. *Eur. J. Biochem.* **1985**, *152*, 299−306.
(32) Wise, D. *Biomaterials and Bioengineering Handbook*; CRC Press: Boca Raton, FL, **2000**
(33) Staros, J.; Write, R.; Swingle, D. *Anal. Biochem.* **1986**, *156*, 220−222.
(34) Tessier, F. J.; Monnier, V. M.; Sayre, L. M.; Kornfied, J. A. *Biochem. J.* **2003**, *369*, 705−719.
(35) Glomb, M.; Monnier, V. M. *J. Biol. Chem.* **1995**, *270*, 10017−10026.
(36) Acharya, A. S.; Manning, J. M. *Proc. Natl. Acad. Sci. U.S.A.* **1983**, *80*, 3590−3594.
(37) Hwang, Y. J.; Granelli, J.; Lyubovitsky, J. G. *Anal. Chem.* **2011**, *83*, 200−206.
(38) Anderson, S. S.; Tsilibary, E. C.; Charonis, A. S. *J. Clin. Invest.* **1993**, *92*, 3045−3052.
(39) Kim, B. M.; Eichler, J.; Reiser, K. M.; Rubenchik, A. M.; Da Silva, L. B. *Laser Surg. Med.* **2000**, *27*, 329−335.
(40) Hwang, Y. J.; Lyubovitsky, J. G. *RSC Anal. Methods* **2011**, *3*, 529−536.
(41) Odetti, P.; Aragno, I.; Rolandi, R.; Garibaldi, S.; Valentini, S.; Cosso, L.; Traverso, N.; Cottalasso, D.; Pronzato, M. A.; Marinari, U. M. *Diabetes Metab. Res. Rev.* **2000**, *16*, 74−81.